



## Multilayer Nano-Structure for Enhanced Sensitivity of Surface Plasmon Resonance Biosensor

TAN TAI NGUYEN<sup>id</sup>

Department of Materials Science, School of Applied Chemistry, Tra Vinh University, Tra Vinh City 87000, Vietnam

Corresponding author: E-mail: nttai60@tvu.edu.vn

Received: 12 March 2024;

Accepted: 19 April 2024;

Published online: 31 May 2024;

AJC-21647

In this work, we demonstrated the figure of merits (FOM) of the plasmonic refractive index sensor using prism based on surface plasmon resonance (SPR). The multilayer structure comprising of the stacked layers of prism/TiO<sub>2</sub>/Ag/MoS<sub>2</sub> with an operating wavelength of near-infrared region used for SPR excitation. It is reported that the optical reflectance spectrum of the SPR sensor can be easily tuned by changing the thicknesses of TiO<sub>2</sub>, Ag and MoS<sub>2</sub> layers. With the optimized thicknesses of the TiO<sub>2</sub>, Ag and MoS<sub>2</sub> layers at 180, 35 and 5 nm, respectively, the findings show that the SPR sensor was obtained at about 102/RIU, which corresponds to a sensor sensitivity of 96.28 %/RIU. This refractive index sensor shows the great sensitivity and detection accuracy by enabling biochemical detection utilizing a small volume of liquid for biological diagnosis.

**Keywords:** Combination, Multilayer, Infrared laser, Sensor, Surface plasmon resonance.

### INTRODUCTION

Biosensors find applications in a wide range of biomedical diagnostics, point-of-care monitoring, food regulation, drug discovery, forensics, *etc.* [1-4]. Recently, several studies have focused on the surface plasmon resonance (SPR) based optical biosensors. The phenomenon known as surface plasmon resonance (SPR) occurs when charge density oscillations are excited at the metal-dielectric interface. Typically, Kretschmann-based SPR biosensors have been fabricated using either optical fiber [5-10] or a thin metal layer applied to the prism [11-15]. By measuring the wavelength or angle at which the SPR condition is fulfilled, one can indirectly determine the change in refractive index of the sensing medium injected to the sensor surface. The SPR waves based on the depth-to-width ratio and the change of wavelength or angle over the refractive index unit in the reflected curve *versus* wavelength or angle can be characterized. Thus, this particular configuration of SPR sensors finds its main application in the field of biology, where it is utilized for various purposes such as the early detection of illnesses like fibrinogen [16-19], glucose [20,21] and foodborne bacterial infections [22-25]. When it comes to efficiency, it is important to mention that the SPR sensor, which utilizes multiple metals, has shown considerable benefits. Dealing with the short penetration depth

of surface plasmon waves and the intense nature of visible light poses certain challenges for setups, as it could potentially harm the biomolecules being targeted. Infrared lasers are fascinating and highly promising technologies that have the potential to overcome these limitations. Recent reports have highlighted the several benefits of SPR sensors that utilize infrared lasers [26-29].

Selecting the appropriate metal layer for the surface is essential to optimize the sensor. Gold is commonly used as a sensor surface coating due to its high chemical stability [30-32], however, the gold coated SPR sensor is somewhat expensive. Another viable material for SPR sensors is silver, which has also demonstrated exceptional sensitivity. On the other hand, the procedure of obtaining an oxidation of silver is most straightforward [33-35]. Furthermore, the utilization of electric materials such as titanium dioxide (TiO<sub>2</sub>), molybdenum oxide (MoO<sub>3</sub>) and zinc oxide (ZnO) has provided significant advantages in the fabrication of surface plasmon resonance (SPR) sensors that utilize visible laser technology [36-38]. These materials offer several benefits since their true permittivity magnitudes are smaller than metals. Recently, MoO<sub>3</sub> has been used as a chemo-resistive sensor to selectively monitor H<sub>2</sub> [37]. This prompts the exploration of a novel sensing platform for surface plasmon resonance (SPR) is based on the multi-layer structures operating at a higher frequency range.

This study aims to improve the features of the sensor by using a new surface plasmon resonance (SPR) structure based on a prism with a three-layer combination. The layers consist of TiO<sub>2</sub>/Ag/molybdenum disulfide (MoS<sub>2</sub>) and are used for detecting foodborne bacteria in the sensing medium. Theoretical modeling and analysis are also offered with a detailed description. The design structure is optimized by varying the thicknesses of silver layers and dielectric materials (TiO<sub>2</sub> and MoS<sub>2</sub>) with refractive index values within the range of 1.33–1.35, which corresponds to *E. coli* concentration of 10<sup>3</sup> cfu/mL [39]. The results demonstrated that utilizing a wavelength of 1064 nm improved the performance of the SPR sensor, specifically enhancing the sensitivity and detection accuracy. This improvement was shown in the combination structure of prism/TiO<sub>2</sub>/Ag/MoS<sub>2</sub>.

### EXPERIMENTAL

The optical sensor (Fig. 1) was designed using a BK7 prism. The proposed multi-layer structure for the semi-conductor layer exposed to sensing fluids with varying refractive indices includes a prism, TiO<sub>2</sub>, Ag and MoS<sub>2</sub>. To protect the Ag layer from oxidation and improve the sensor's sensitivity, MoS<sub>2</sub> was applied on top of it. High efficiency in light trapping for plasmonic excitation was achieved with the inclusion of a TiO<sub>2</sub> layer, which improved adhesion between the plasmonic silver layer and the prism [36].

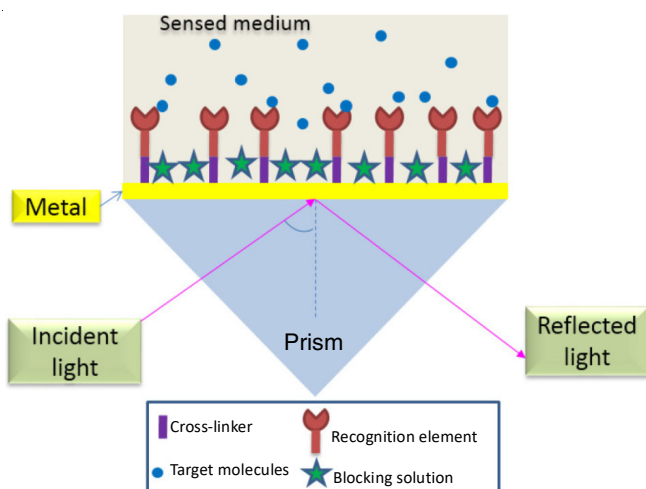


Fig. 1. Sketch of the proposed sensor comprising of the stacked layers

A collimated beam of 1064 nm infrared light flowing through a polarizer was used to generate incident light with transverse magnetic (TM) polarization, which in turn excites surface plasmon waves. It was an optical detector that gathered the reflected light. This simulation parameters can be run for the multi-layer optical sensor are listed in Table-1.

Transfer matrix regression is used to evaluate the reflection coefficient for the multilayer model of the sensor structure (Fig. 1). The relationship in this model between the tangential field components at the first and last interfaces is shown below [43]:

$$\begin{bmatrix} E_{t1} \\ H_{t1} \end{bmatrix} = M \begin{bmatrix} E_{t3} \\ H_{t3} \end{bmatrix}$$

Materials	Wavelength (nm)	Dielectric constant ( $\epsilon_r + \epsilon_i$ )	Ref.
Prism (BK7)	1064	2.28	[33]
Ag	1064	-66.26 + 5.83i	[40]
MoS <sub>2</sub>	1064	4.32	[41]
TiO <sub>2</sub>	1064	6.15	[42]

where  $E_{t1}$  and  $H_{t1}$  represent the electric and magnetic field components at the first interface between TiO<sub>2</sub> and Ag. Similarly,  $E_{t3}$  and  $H_{t3}$  represent the electric and magnetic field components at the third interface, which is the interface between MoS<sub>2</sub> and the sensing medium. In addition, the N-layer combined characteristic matrix is denoted as M and is provided below:

$$M = \prod_{k=2}^{N-1} M_k = \begin{bmatrix} M_{11} & M_{12} \\ M_{21} & M_{22} \end{bmatrix}$$

$$\text{where, } M_k = \begin{bmatrix} \cos \beta_k & (-i/q_k) \sin \beta_k \\ -iq_k \sin \beta_k & \cos \beta_k \end{bmatrix}$$

$$q_k = \frac{(\epsilon_k - \epsilon_{\text{BK7}} \sin^2 \phi)^{1/2}}{\epsilon_k}$$

$$\beta_k = \frac{2\pi d_k}{\lambda} (\epsilon_k - \epsilon_{\text{BK7}} \sin^2 \phi)^{1/2}$$

The reflection coefficients of transverse magnetic (TM) field (*p*-polarization) and its amplitudes are given as below, respectively.

$$r_q = \frac{(M_{11} + M_{12}q_s) + q_{\text{BK7}} - (M_{21} + M_{22}q_s)}{(M_{11} + M_{12}q_s) + q_{\text{BK7}} + (M_{21} + M_{22}q_s)},$$

$$R = |r_p|^2$$

where  $k = k^{\text{th}}$  layer;  $d_k =$  thickness of  $k^{\text{th}}$  layer;  $\epsilon_{\text{BK7}} =$  dielectric constant of prism;  $\epsilon_k =$  dielectric constant of  $k^{\text{th}}$  layer;  $\phi =$  incident angle of laser light;  $\lambda =$  wavelength of laser;  $\epsilon_s =$  dielectric constant of the sensing medium.

The SPR characterization was conducted by analyzing the reflectance *versus* incidence angle plot of the laser light after it was reflected from the sensor surface. The resonant angle is the angle where the reflectance is lowest. The resonant angle and lowest reflectance are contingent upon the excitation wavelength as well as the thicknesses of metal (Ag), semiconductor (MoS<sub>2</sub>) and dielectric (TiO<sub>2</sub>) layers. Additionally, they are influenced by the refractive index of the sensing medium (water). The study focused on optimizing the sensor structure by investigating the thicknesses of all layers, including Ag, MoS<sub>2</sub> and TiO<sub>2</sub>, in response to changes in the refractive index of the sensing medium. Based on the simulated results on the relationship between reflectance and incident angle, the sensor sensitivity and accuracy of the dip in the reflectance curve have been determined as shown below :

$$S = \frac{\delta\phi}{\delta n} \quad (11)$$

$$DL = \frac{1}{FWHM} \tag{12}$$

$$FOM = D \times S \tag{13}$$

where S = sensor sensitivity and n = refractive index of sensing medium; DL = detection limit and FWHM = full-width at half-maximum; D = depth in the reflectance curve;  $\epsilon'_m$  = real part of the dielectric constant of metal layer.

**RESULTS AND DISCUSSION**

The majority of recent studies have been primarily concerned with optimizing the thickness of the metal layer. It has been proven that the thickness of metal layer is highly influenced by the structure of sensor. In this investigation, the thickness of silver layer was fine-tuned within a range of 30-60 nm, with increments of 5 nm. This was done while subjecting the layer to an IR laser with a wavelength of 1064 nm. Fig. 2 displays the SPR characterisation curve, which takes into account the BK7 prism coated with a thin coating of silver and covered by distilled water as the sensing medium, with a refractive index of 1.33 (RIU). Fig. 2b demonstrates a modest variation in the resonant angle as a result of altering the thickness of the metal

layer. Furthermore, the reflectivity dip of the surface plasmon resonance (SPR) curve does vary as a result of alterations in the thickness of silver layer. The optimal thickness of silver layer was determined by analyzing the reflectivity dip with the highest value or the reflectance approaching zero at the resonant angle, which corresponds to the angle at which the majority of electromagnetic wave energy is transferred to the surface plasmon wave.

Fig. 2a displayed the SPR characteristic curve-based prediction of the reflectivity strength. According to the results, the ideal thickness of silver is around 35 nm when the resonance angle is 64.2° (Fig. 2b). One parameter used to determine the ideal silver layer thickness is the sensor sensitivity. Refractive index of the sensing medium was adjusted from 1.33 to 1.351 (RIU), which corresponds to 10<sup>3</sup> cfu/mL shift from deionized water to *E. coli* [39]. Fig. 2c shows the estimated sensitivity of 95 °/RIU for the prism/Ag sensor and it should be mentioned that the sensitivity of the sensor was measured by dividing the change in the sensing medium’s refractive index by the changing the resonant angle. Furthermore, the thickness of the silver layer was linked to the energy transfer and increasing the thickness of the silver layer resulted in an increase in energy transmission, as illustrated in Fig. 2d. Maximum energy transfer of

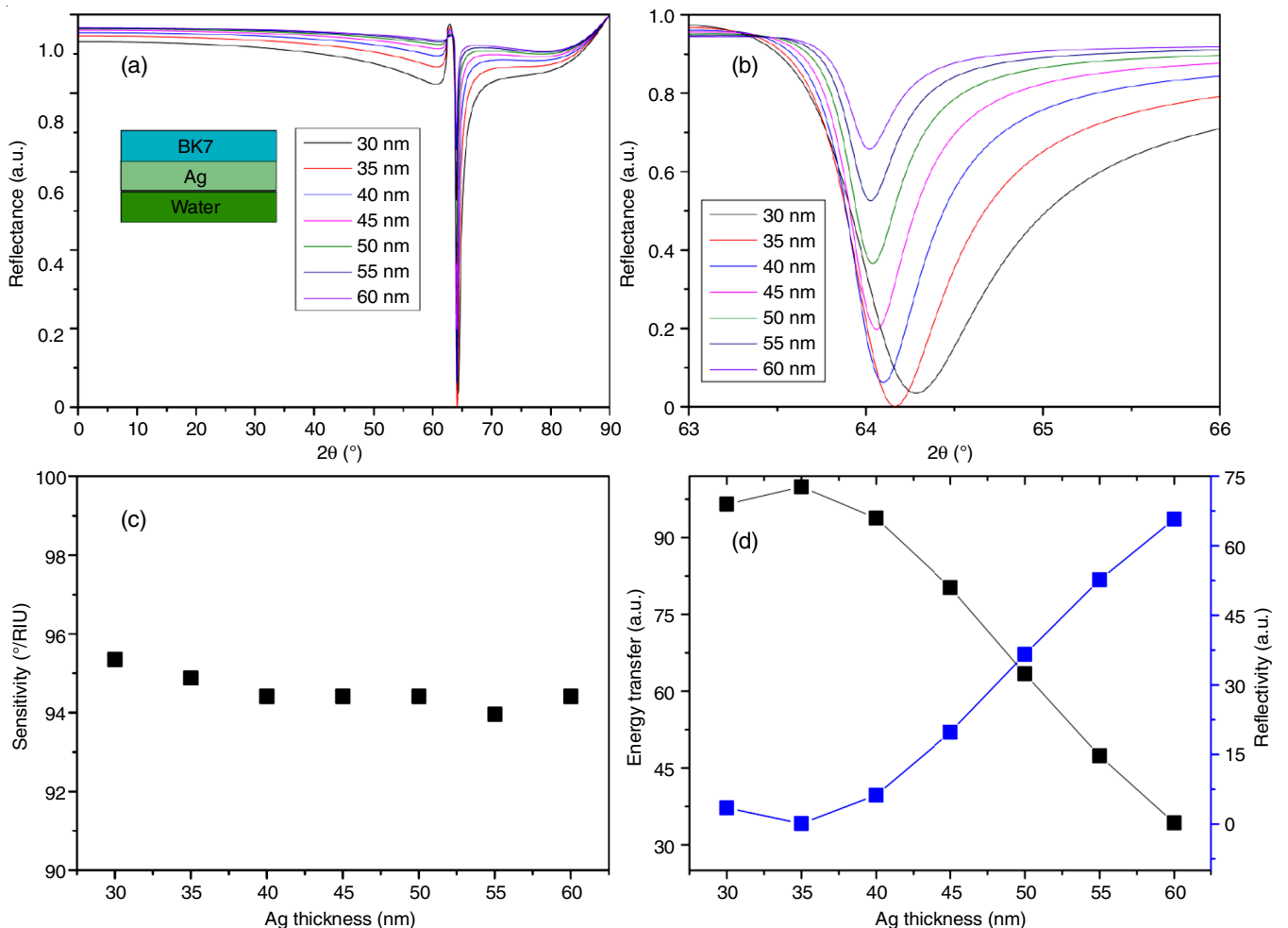


Fig. 2. (a) Simulated results of Ag thickness changed from 30 to 60 nm; (b) the magnified view of (a) from 63 to 66 degree; (c) sensor sensitivity versus the Ag thickness; (d) energy transfer versus the Ag thickness

99.78 a.u. was achieved at a resonant angle of  $64.2^\circ$  and an optimum thickness of 35 nm for Ag.

The sensor structure was enhanced by incorporating a  $\text{TiO}_2$  layer between the silver layer and the BK7 substrate. The ideal thickness of the Ag layer was 35 nm. Fig. 3a-b displayed the SPR characteristic curve for various  $\text{TiO}_2$  thicknesses (80–260 nm, with a 20 nm enhancement) based on the sensor structure of BK7/ $\text{TiO}_2$ /Ag/sensing medium. The SPR resonant angle remained unchanged, however, a slight shift in the SPR curve's contrast was observed. A correlation between the thickness of the  $\text{TiO}_2$  layer and the sensitivity was observed. Fig. 3c shows that the maximum sensor sensitivity was achieved between 160 and 180 nm and the energy transfer, though, was linked to the  $\text{TiO}_2$  thickness. The energy transfer is enhanced as the  $\text{TiO}_2$  thickness increases, thus with a  $\text{TiO}_2$  thickness of 180 nm, the maximum energy transfer was 99.95 a.u. and also  $\text{TiO}_2$  layer improves the sensitivity of the sensor, which makes the silver layer stick to the prism more effectively.

The results were utilized to determine the thickness of  $\text{MoS}_2$  layer, which was based on the 35 nm thickness of Ag and 180 nm thickness of  $\text{TiO}_2$ . In order to maximize the accuracy and efficiency for a given thickness of Ag and  $\text{TiO}_2$ , the thickness of  $\text{MoS}_2$  from 5 to 30 nm was scanned. The reflectance for

different  $\text{MoS}_2$  thickness is shown in Fig. 4 and it was found that the SPR dip shifted slightly toward and the reflectance rose when the  $\text{MoS}_2$  thickness was increased. These findings allowed for the estimation of accuracy, sensitivity and other parameters of the sensor. Fig. 4b shows the results showing that the sensor sensitivity increased as the  $\text{MoS}_2$  thickness increased.

By fitting the estimated results in Fig. 5 to the ideal characteristic parabolic relation for the sensor sensitivity with shifting the  $\text{MoS}_2$  thickness throughout operation, the parabolic shape with a quadratic second order equation ( $S = S_0 + Ax + Bx^2$ ) was determined. The findings demonstrated that the  $\text{MoS}_2$  layer had a minimum sensitivity of around  $100.23^\circ/\text{RIU}$  for the multilayer structure-based sensor operating ( $S_0$ ) (Table-2). Additionally, the results demonstrated that the optimal sensor sensitivity of  $157.21^\circ/\text{RIU}$  would have risen by 63.54% compared to not using the  $\text{MoS}_2$  layer (with a thickness of 30 nm). With sensitivity enhancements of 1.01%, 6.31%, 13.68%, 24.21% and 39.95% respectively, this sensitivity outperformed that of the other cases utilizing different thickness of the  $\text{MoS}_2$  layer, namely 5 nm, 10 nm, 15 nm, 20 nm and 25 nm. In addition, the second order quadratic model, which was suggested, matched the estimated data well, since the correlation coefficient ( $R^2$ ) was greater than 0.98.

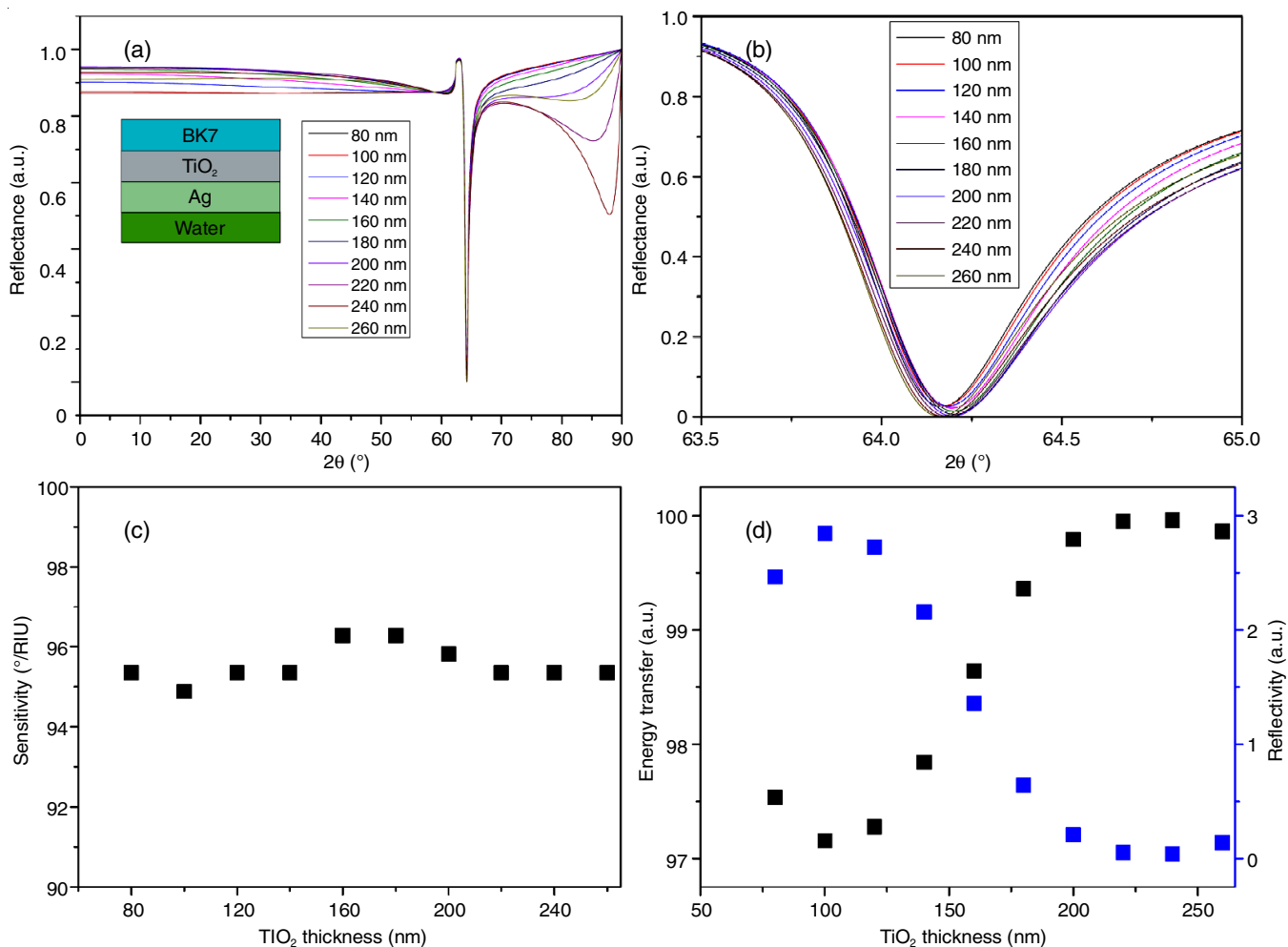


Fig. 3. (a) Simulated results of  $\text{TiO}_2$  thickness changed from 80 to 260 nm based on sensor structure of BK7/ $\text{TiO}_2$ /Ag/sensing medium; (b) the magnified view of (a), (c) sensor sensitivity *versus* the  $\text{TiO}_2$  thickness; (d) energy transfer *versus* the  $\text{TiO}_2$  thickness

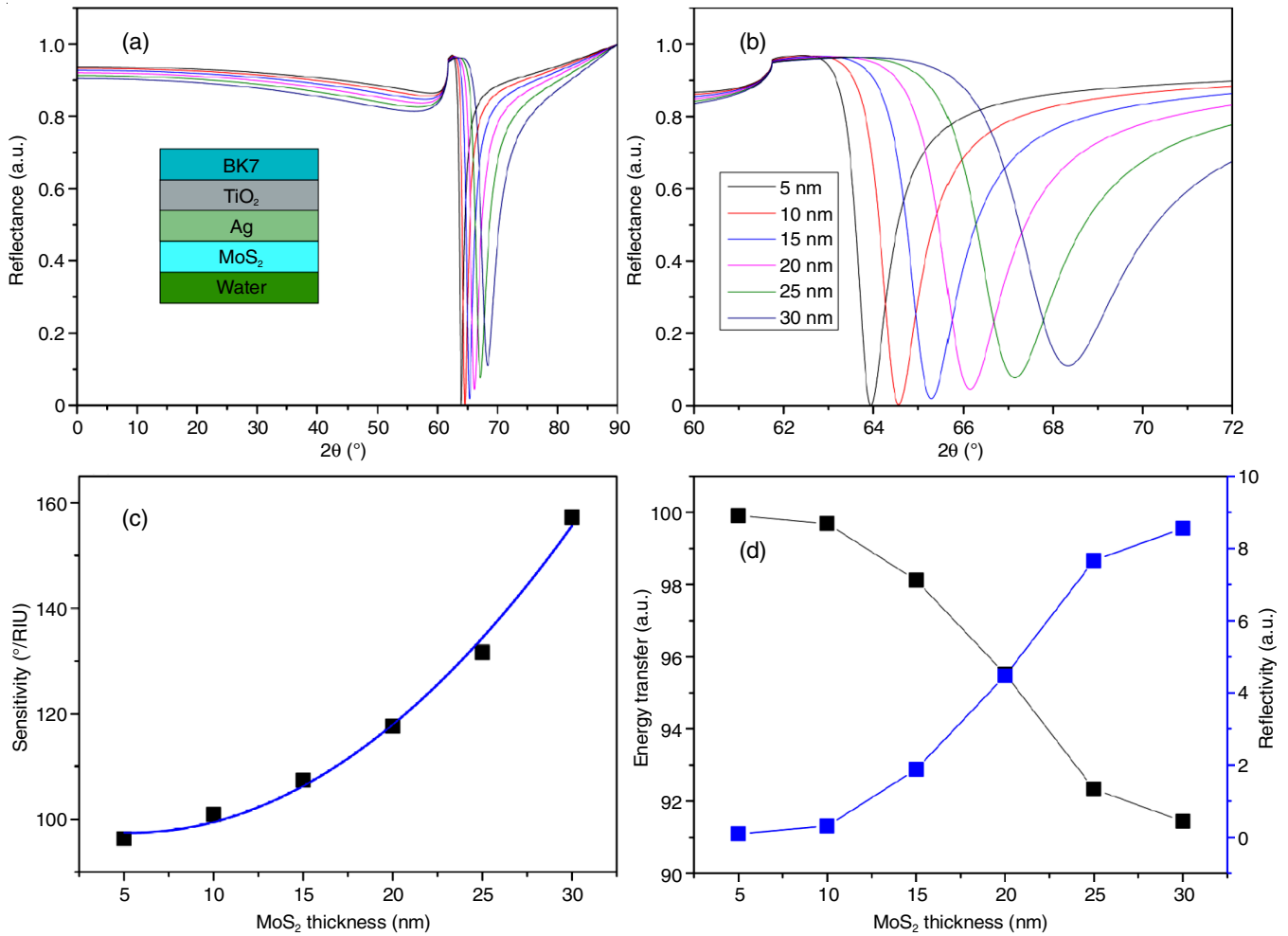


Fig. 4. SPR spectra for varying thicknesses of MoS<sub>2</sub> based on the sensor structure of BK7/TiO<sub>2</sub>/Ag/MoS<sub>2</sub>/sensing medium; (b) magnified view of (a) from 60 to 72°, (c) Sensor sensitivity *versus* the MoS<sub>2</sub> thickness; (d) energy transfer *versus* the MoS<sub>2</sub> thickness

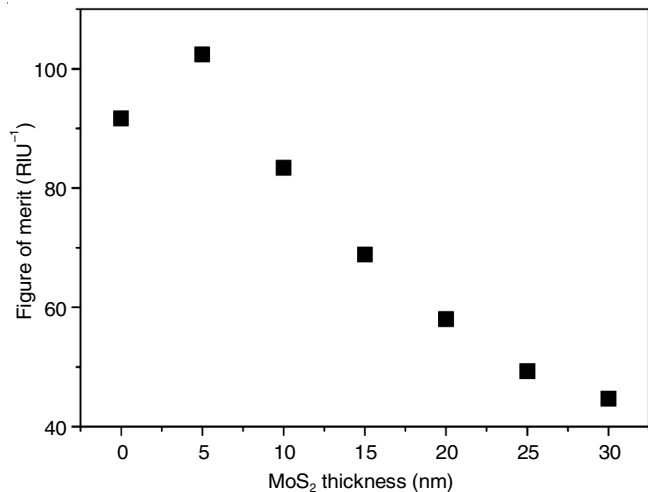


Fig. 5. Comparison of FOM of the sensor performance as MoS<sub>2</sub> thicknesses

According to this model, the sensing ability improves as the thickness of MoS<sub>2</sub> layer increases. Nevertheless, a reflectance increase of almost 80% was achieved by MoS<sub>2</sub> layer growth of more than 30 nm. Since the reflectivity was 20% higher, the surface plasmon resonance was not strongly generated by the coupling effect of transverse magnetic waves and evanescent waves. This resulted in a lower FOM value (Fig. 5) and with a 5 nm MoS<sub>2</sub> layer thickness, the highest FOM was achieved at around 102/RIU. This result demonstrates an improvement of 5.5 times compared to a plasmonic gold coating [44]. It is remarkable that the FOM value obtained with a MoS<sub>2</sub> thickness of 5 nm was 12.09% and 160.67% higher than without the MoS<sub>2</sub> layer and 30 nm MoS<sub>2</sub> layer thickness, respectively, as depicted in Fig. 5. Substrates based on BK7-glass can be utilized in SPR sensors with a multilayer structure of [TiO<sub>2</sub>(140 nm)/Ag (60 nm)/MoS<sub>2</sub> (5 nm)]. Improving the FOM and sensor sensitivity by increasing the depth to which the evanescent field penetrates the sensing medium allows for the detection of small concentrations of biological agents.

There are a number of advantages to using silver in conjunction with other materials, such as TiO<sub>2</sub> and MoS<sub>2</sub>, to develop an SPR sensor that operates at 1064 nm. Compared to SPR sensors made with more costly materials, such as gold, those based on

	Sensor sensitivity, S <sub>0</sub> (°/RIU)	Fitting coefficients		
		A	B	R <sup>2</sup>
MoS <sub>2</sub>	100.23	-1.03	0.09	0.99

a combination of TiO<sub>2</sub>/Ag/MoS<sub>2</sub> have superior sensor sensitivity. Furthermore, sandwiching TiO<sub>2</sub> between the prism and the silver layer may result in improved detection accuracy, implying that the sensor's ability in detecting bio-sensing can be repeated. The simulated results demonstrated the viability of using combination materials with IR laser excitation for SPR sensors, opening up new research possibilities for bio-sensing applications.

## Conclusion

This study conducted a numerical evaluation of the surface plasmon resonance (SPR) sensor. The sensor construction consisted of a prism/TiO<sub>2</sub>/Ag/MoS<sub>2</sub> configuration and operated at a wavelength of 1064 nm. The resonant spectra can be effectively achieved by precisely altering the thicknesses of TiO<sub>2</sub>, Ag and MoS<sub>2</sub> layers. The figure of merit (FOM) of the sensor under consideration reached about 102/RIU, indicating a sensor sensitivity of 96.28 °RIU. This was obtained by optimizing the thickness of TiO<sub>2</sub>, Ag and MoS<sub>2</sub> layers to 180 nm, 35 nm, and 5 nm, respectively. The constructed SPR sensor is expected to be suitable for different applications, including the quantitative detection of biomolecules with improved performance indicators.

## ACKNOWLEDGEMENTS

This research was supported by Tra Vinh University under Basic Science Research.

## CONFLICT OF INTEREST

The authors declare that there is no conflict of interests regarding the publication of this article.

## REFERENCES

- H.J. Watts, C.R. Lowe and D.V. Pollard-Knight, *Anal. Chem.*, **66**, 2465 (1994); <https://doi.org/10.1021/ac00087a010>
- M.A. Cooper, *Nat. Rev. Drug Discov.*, **1**, 515 (2002); <https://doi.org/10.1038/nrd838>
- A.J. Haes, L. Chang, W.L. Klein and R.P. Van Duyne, *J. Am. Chem. Soc.*, **127**, 2264 (2005); <https://doi.org/10.1021/ja044087q>
- Y. Yanase, A. Araki, H. Suzuki, T. Tsutsui, T. Kimura, K. Okamoto, T. Nakatani, T. Hiragun and M. Hide, *Biosens. Bioelectr.*, **25**, 1244 (2010); <https://doi.org/10.1016/j.bios.2009.09.042>
- E. Kretschmann and H. Raether, *Z. Naturforschung A*, **23**, 2135 (1968); <https://doi.org/10.1515/zna-1968-1247>
- S.Y. Wu, H.P. Ho, W.C. Law, C. Lin and S.K. Kong, *Optics Lett.*, **29**, 2378 (2004); <https://doi.org/10.1364/OL.29.002378>
- O. Telezhnikova and J. Homola, *Optics Lett.*, **31**, 3339 (2006); <https://doi.org/10.1364/OL.31.003339>
- J. Li, D. Han, J. Zeng, J. Deng, N. Hu and J. Yang, *Optics Expr.*, **28**, 9 (2020); <https://doi.org/10.1364/OE.389226>
- A. Paliwal, R. Gaur, A. Sharma, M. Tomar and V. Gupta, *Optik*, **127**, 7642 (2016); <https://doi.org/10.1016/j.ijleo.2016.05.103>
- A. Leung, P.M. Shankar and R. Mutharasan, *Sens. Actuators B: Chemical*, **125**, 688 (2007); <https://doi.org/10.1016/j.snb.2007.03.010>
- R.K. Verma, A.K. Sharma and B.D. Gupta, *Optics Commun.*, **281**, 1486 (2008); <https://doi.org/10.1016/j.optcom.2007.11.007>
- T.T. Nguyen, E.-C. Lee and H. Ju, *Optics Expr.*, **22**, 5590 (2014); <https://doi.org/10.1364/OE.22.005590>
- T.T. Nguyen, S.O. Bea, D.M. Kim, W.J. Yoon, J.-W. Park, S.S.A. An and H. Ju, *Int. J. Nanomed.*, **10**, 155 (2015); <https://doi.org/10.2147/IJN.S88963>
- H. Zhang, X. Zhou, X. Li, P. Gong, Y. Zhang and Y. Zhao, *Biosensors*, **13**, 405 (2023); <https://doi.org/10.3390/bios13030405>
- A.P. Abel, M.G. Weller, G.L. Duveneck, M. Ehrat and H.M. Widmer, *Anal. Chem.*, **68**, 2905 (1996); <https://doi.org/10.1021/ac960071+>
- Y.E. Monfared, *Biosensors*, **10**, 77 (2020); <https://doi.org/10.3390/bios10070077>
- J. Kim, S. Kim, T.T. Nguyen, R. Lee, T. Li, C. Yun and H. Ju, *J. Electron. Mater.*, **45**, 2354 (2016); <https://doi.org/10.1007/s11664-015-4292-5>
- T.T.V. Nu, N.H.T. Tran, E. Nam, T.T. Nguyen, W.J. Yoon, S. Cho, J. Kim, K.-A. Chang and H. Ju, *RSC Adv.*, **8**, 7855 (2018); <https://doi.org/10.1039/C7RA11637C>
- D.E. Souto, J. Volpe, C.D.C. Gonçalves, C.H. Ramos and L.T. Kubota, *Talanta*, **205**, 120122 (2019); <https://doi.org/10.1016/j.talanta.2019.120122>
- S.K. Srivastava and I. Abdulhalim, *J. Biosens. Bioelectron.*, **6**, 172 (2015); <https://doi.org/10.4172/2155-6210.1000172>
- N. Mudgal, A. Saharia, A. Agarwal, J. Ali, P. Yupapin and G. Singh, *Opt. Quantum Electron.*, **52**, 307 (2020); <https://doi.org/10.1007/s11082-020-02427-0>
- J.W.F. Law, N.S.A. Mutalib, K.G. Chan and L.H. Lee, *Front. Microbiol.*, **5**, 122692 (2015); <https://doi.org/10.3389/fmicb.2014.00770>
- A. Rohde, J.A. Hammerl, I. Boone, W. Jansen, S. Fohler, G. Klein, R. Dieckmann and S. Al Dahouk, *Trends Food Sci. Technol.*, **62**, 113 (2017); <https://doi.org/10.1016/j.tifs.2017.02.006>
- B. Priyanka, R.K. Patil and S. Dwarakanath, *Indian J. Med. Res.*, **144**, 327 (2016); <https://doi.org/10.4103/0971-5916.198677>
- T.T. Nguyen, K.T.L. Trinh, W.J. Yoon, N.Y. Lee and H. Ju, *Sens. Actuators B Chem.*, **242**, 1 (2017); <https://doi.org/10.1016/j.snb.2016.10.137>
- R. Jha and A.K. Sharma, *Opt. Lett.*, **34**, 749 (2009); <https://doi.org/10.1364/OL.34.000749>
- A.K. Pandey and A.K. Sharma, *Photon. Nanostructures*, **28**, 94 (2018); <https://doi.org/10.1016/j.photonics.2017.12.003>
- N. Van Sau, Q.M. Ngo, T.B. Phan, N.Q. Tran and T.T. Nguyen, *J. Electron. Mater.*, **49**, 7420 (2020); <https://doi.org/10.1007/s11664-020-08384-4>
- N. Van Sau, M.T. Hoa, N.X.T.D. Trinh and N.T. Tai, *Dalat Univ. J. Sci.*, **11**, 56 (2021); [https://doi.org/10.37569/DalatUniversity.11.1.775\(2021\)](https://doi.org/10.37569/DalatUniversity.11.1.775(2021))
- N. Bhalha, P.K. Sharma and S. Chakrabarti, *ACS Omega*, **7**, 27664 (2022); <https://doi.org/10.1021/acsomega.2c03326>
- A.K. Sharma and B.D. Gupta, *Photon. Nanostructures*, **3**, 30 (2005); <https://doi.org/10.1016/j.photonics.2005.06.001>
- A. Argyros, N. Issa, I. Bassett and M.A. van Eijkelenborg, *Opt. Lett.*, **29**, 20 (2004); <https://doi.org/10.1364/OL.29.000020>
- M. Iga, A. Seki and K. Watanabe, *Sens. Actuators B Chem.*, **101**, 368 (2004); <https://doi.org/10.1016/j.snb.2004.04.007>
- J. Wang, D. Song, L. Wang, H. Zhang, H. Zhang and Y. Sun, *Sens. Actuators B Chem.*, **157**, 547 (2011); <https://doi.org/10.1016/j.snb.2011.05.020>
- L. Wang, Y. Sun, J. Wang, X. Zhu, F. Jia, Y. Cao, X. Wang, H. Zhang and D. Song, *Talanta*, **78**, 265 (2009); <https://doi.org/10.1016/j.talanta.2008.11.019>
- T. Arai, P.K.R. Kumar, C. Rockstuhl, K. Awazu and J. Tominaga, *J. Opt. A, Pure Appl. Opt.*, **9**, 699 (2007); <https://doi.org/10.1088/1464-4258/9/7/022>

37. A.R. Shafieyan, M. Ranjbar and P. Kameli, *Int. J. Hydrogen Energy*, **44**, 18628 (2019); <https://doi.org/10.1016/j.ijhydene.2019.05.171>
38. R. Tabassum and B.D. Gupta, *Biosens. Bioelectron.*, **91**, 762 (2017); <https://doi.org/10.1016/j.bios.2017.01.050>
39. Y. Saad, M. Selmi, M.H. Gazzah and H. Belmabrouk, *Eur. Phys. J. Appl. Phys.*, **82**, 31201 (2018); <https://doi.org/10.1051/epjap/2018180059>
40. W.S.M. Werner, K. Glantschnig and C. Ambrosch-Draxl, *J. Phys. Chem. Ref. Data*, **38**, 1013 (2009); <https://doi.org/10.1063/1.3243762>
41. V.G. Kravets, F. Wu, G.H. Auton, T. Yu, S. Imaizumi and A.N. Grigorenko, *NPJ 2D Mater. Appl.*, **3**, 36 (2019); <https://doi.org/10.1038/s41699-019-0119-1>
42. J.R. DeVore, *J. Opt. Soc. Am.*, **41**, 416 (1951); <https://doi.org/10.1364/JOSA.41.000416>
43. B.D. Gupta and A.K. Sharma, *Sens. Actuators B Chem.*, **107**, 40 (2005); <https://doi.org/10.1016/j.snb.2004.08.030>
44. Q. Wang, X. Jiang, L.Y. Niu and X.C. Fan, *Opt. Lasers Eng.*, **128**, 105997 (2020); <https://doi.org/10.1016/j.optlaseng.2019.105997>